Accepted Manuscript

Compounds *N,N′*-bis(9-cyclohexyl-9-xanthenyl)ethylenediamine and its thio derivative, *N,N′*-bis(9-cyclohexyl-9-thioxanthenyl)ethylenediamine, as potential hosts in the presence of xylenes and ethylbenzene: Conformational analyses and molecular modelling considerations

Benita Barton, Ulrich Senekal, Eric C. Hosten

Please cite this article as: Barton B, Senekal U, Hosten EC, Compounds *N,N′*-bis(9-cyclohexyl-9-xanthenyl)ethylenediamine and its thio derivative, *N,N′*-bis(9-cyclohexyl-9-thioxanthenyl)ethylenediamine, as potential hosts in the presence of xylenes and ethylbenzene: Conformational analyses and molecular modelling considerations, *Tetrahedron* (2019), doi: https://doi.org/10.1016/j.tet.2019.04.065.
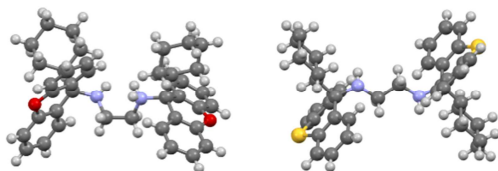
GRAPHICAL ABSTRACT

Compounds *N,N'*-bis(9-cyclohexyl-9-xanthenyl)ethylenediamine and its thio derivative, *N,N'*-bis(9-cyclohexyl-9-thioxanthenyl)ethylenediamine, as potential hosts in the presence of xylenes and ethylbenzene: conformational analyses and molecular modelling considerations

Benita Barton,* Ulrich Senekal and Eric C. Hosten

Department of Chemistry, PO Box 77000, Nelson Mandela University, Port Elizabeth, 6031, South Africa. E-mail: benita.barton@mandela.ac.za

Compounds *N,N'*-bis(9-cyclohexyl-9-xanthenyl)ethylenediamine and its thio derivative, *N,N'*-bis(9-cyclohexyl-9-thioxanthenyl)ethylenediamine, as potential hosts in the presence of xylenes and ethylbenzene: conformational analyses and molecular modelling considerations

Benita Barton,* Ulrich Senekal and Eric C. Hosten

Department of Chemistry, PO Box 77000, Nelson Mandela University, Port Elizabeth, 6031, South Africa. E-mail: benita.barton@mandela.ac.za

Abstract

Two novel crystalline compounds, *N,N'*-bis(9-cyclohexyl-9-xanthenyl)ethylenediamine (OED) and its thio derivative, *N,N'*-bis(9-cyclohexyl-9-thioxanthenyl)ethylenediamine (SED), were designed and synthesized in our laboratories, and assessed for their potential as host compounds for the four C8 aromatic compounds, namely *o*-, *m*- and *p*- xylene (*o*-Xy, *m*-Xy, *p*-Xy), and ethylbenzene (EB). Despite the only difference between the two compounds being the heteroatoms in their B rings, immense behaviour differences were noted: only OED displayed host behaviour in these conditions, clathrating all but *m*-Xy, while SED failed to form complexes with any of the four organic solvents. These observations prompted an investigation into the conformations of OED and SED through single crystal diffraction (SCXRD) analyses as well as computational studies with surprising results. SCXRD was also employed to analyse the three complexes that successfully formed with OED, and thermal analyses (TA) assisted in understanding the selectivity behaviour of OED when presented with mixed guests.

Keywords

Host-guest Chemistry; Supramolecular Chemistry; Xanthenyl; Xylene; Ethylbenzene.

1. Introduction

Host-guest chemistry is a field of science that is characterized by non-covalent interactions between at least two different molecular compounds, namely the host and the guest,[1,2] and may be subdivided into two major classes known as the clathrands and the cavitands. Cavitands are those host compounds that contain permanent intramolecular cavities, and guests are able to interact with the host both in solution and in the crystalline state. Clathrands, on the other hand, only possess extramolecular cavities which are present only in the crystalline or solid states.[3] The non-covalent forces that are responsible for entrapping the guest within the host crystal are, more usually, hydrogen bonding, ion pairing (ion···ion, dipole···dipole, ion···dipole), π···π, C–H···π, and van der Waals interactions.[1–4] A few examples of cavitands include the calixarenes, carcerands, cyclodextrins, cyclophanes, cryptophanes, crown ethers and cryptands, while typical clathrands are the hexa-, roof, scissor, urea and wheel-and-axle hosts.[4] Chemistry of this type has a number of applications in fields such as the chemical, biological and pharmaceutical industries, and include the separation of enantiomers and other isomers,[5] chromatography,[6,7] employment in stationary phases for chromatographic separations,[4,6] storage of toxic substances and gases,[3] and various environmental applications,[7] amongst numerous others.

Owing to the challenges associated with the separation of the components of the C8 aromatic fraction through distillation [*o*-, *m*-, *p*- xylene and ethylbenzene (*o*-Xy, *m*-Xy, *p*-Xy, EB), Scheme 1] due to their near-identical physical properties (boiling points: *o*-Xy 144.5 °C, *m*-Xy 139.1 °C, *p*-Xy 138.2 °C, EB 136.2 °C), alternative methods for their separation are attractive. To this end, many researchers have spent much time and capacity on investigating this challenge. As early as the 1950s, Clark *et al*[8] examined the separation of these compound types by means of the formation of a 1:1 solid *p*-Xy:CCl$_4$ complex from a ternary mixture containing this xylene and the *meta* isomer. Schaeffer and his co-workers[9] also considered complex formation but using inorganic compounds as complexing material. Other strategies have employed zeolites,[10] gas chromatography,[11,12] and metal-organic frameworks comprising vanadium(IV) in the

structure,[13] while Lusi and Barbour made use of a nickel-based Werner complex in their work.[14] Organic host-guest chemistry has also been considered here, and calixarenes have been shown to behave selectively in the presence of these compounds during crystallization experiments.[15] Furthermore, Toda *et al*[16] demonstrated that the host compound 1,1,2,2-tetraphenylethane-1,2-diol possesses the ability to selectively include *p*-Xy from a *p*-Xy/*m*-Xy mixture, and Nassimbeni and co-workers[17] employed host compounds 9,9'-bianthryl, 9,9'-spirobifluorene and *trans*-2,3-dibenzoylspiro[cyclopropane-1,9-fluorene] to achieve this separation. A recent review commendably summarises much of the work that has taken place in the area of the xylene separations.[18]

During ongoing investigations in our laboratories that focusses on this challenge, we reported that a tartaric acid-derived host compound, (*R*,*R*)-(−)-2,3-dimethoxy-1,1,4,4-tetraphenylbutane-1,4-diol, was able to extract only moderate amounts (54%) of *p*-Xy from a ternary mixture of the xylenes,[19] while *N*,*N'*-bis(9-phenyl-9-thioxanthenyl)ethylenediamine fared significantly better, and 95% of the same isomer was observed in the crystals that emanated during the recrystallization process.[20] The success of this latter host prompted further examination and, consequently, novel host derivatives were prepared based on a substitution of the ethylenediamine linker for a *trans*-cyclohexane-1,4-diamine one, and this afforded two compounds, namely *trans*-*N*,*N'*-bis(9-phenyl-9-xanthenyl)cyclohexane-1,4-diamine and *trans*-*N*,*N'*-bis(9-phenyl-9-thioxanthenyl)cyclohexane-1,4-diamine.[21] The recrystallization of these from a quaternary *o*-Xy/*m*-Xy/*p*-Xy/EB mixture showed that both hosts were efficient and displayed selectivity for the *para* isomer once more (74 and 71%, respectively).

Owing to the encouraging results obtained for the xanthenyl-type systems, in the present work we have further modified these structures to afford two novel species, *N*,*N'*-bis(9-cyclohexyl-9-xanthenyl)ethylenediamine (OED) and *N*,*N'*-bis(9-cyclohexyl-9-thioxanthenyl)ethylenediamine (SED), and examined their behaviour in this context (Scheme 1). We were surprised to observe that, despite the only difference between the two compounds being the heteroatom in their B rings, OED and SED displayed very different host ability when presented with these guest types.

In fact, SED did not function as a host and was not able to form complexes with any of the four organic solvents, while OED was very capable, with the exception of *m*-Xy, which OED did not clathrate. This surprising observation prompted an in-depth analysis into the conformations of the two compounds, both in their crystal structures and through molecular modelling, in order to elucidate the reasons for the immense host behaviour differences. All successfully-formed single solvent complexes were also subjected to SCXRD and thermal analyses and these assisted in explaining the selective behaviour that OED displayed when recrystallized from various mixtures of these organic solvents. We now report on these findings.
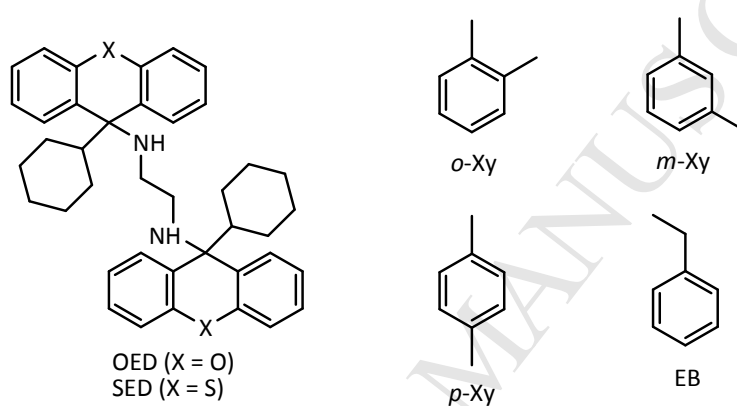
Scheme 1. Structures of host *N,N′*-bis(9-cyclohexyl-9-xanthenyl)ethylenediamine (OED) and *N,N′*-bis(9-cyclohexyl-9-thioxanthenyl)ethylenediamine (SED), and guests *o*-xylene (*o*-Xy), *m*-xylene (*m*-Xy), *p*-xylene (*p*-Xy) and ethylbenzene (EB).

2. Experimental

2.1 General

All starting materials and solvents were purchased from Merck and used without further purification. The melting points of all synthesized solids were measured on a Stuart SMP10 melting point apparatus and are uncorrected. The ^{1}H- and ^{13}C- NMR spectra were recorded by means of a 400 MHz Bruker 400 Ultrashield Plus spectrometer, and CDCl$_3$ was used as the deuterated solvent. These spectra were analyzed using Bruker TopSpin 3.2 data software. The

infrared spectra were obtained by means of a Bruker Tensor 27 FT-IR spectrometer. All spectra are provided in the Supplementary Information section (Figures S1–S6).

GC-MS was an appropriate method with which to analyse complexes that were crystallized from mixed guests. This was achieved by means of an Agilent 7890A gas chromatograph fitted with an Agilent 5975C VL mass spectrometer, equipped with an Agilent J&W Cyclosil-B column. An initial temperature of 50 °C was continued for 1 min, which was followed by a heating ramp of 0.5 °C·min^{-1} until 60 °C was reached, and the temperature was maintained there for 1 min.

SCXRD experiments were conducted on suitable crystals of apohosts OED and SED, and the three single solvent complexes with OED (2OED•*o*-Xy, 2OED•*p*-Xy and 2OED•EB). These data were obtained at 200 K using a Bruker Kappa Apex II diffractometer utilizing a graphite-monochromated Mo Kα radiation (λ = 0.71073 Å), and analysed by means of APEXII data software, while the SAINT program was used for data reduction and cell refinement.[22] The structures were solved using SHELXT-2018.[23] SHELXL-2018,[24] with SHELXLE[25] as a graphical interface, was used to refine the structures by employing least-squares methods. All atoms, excluding hydrogen, were refined anisotropically. Absorption effects present in the data were corrected for using SADABS.[22] These crystal structures were deposited at the Cambridge Crystallographic Data Centre, and CCDC numbers are as follows: 1895818 (OED), 1895819 (SED), 18958202 (OED•*o*-Xy), 1895821 (2OED•*p*-Xy) and 1895822 (2OED•EB). The Mercury 3.10.2 software package[26] was used to construct figures displaying the host–guest packing as well as for calculating voids present in the crystal after removal of the guest from the packing calculation.

DSC and TG experiments were conducted on all of the complexes synthesized in this work. These thermal data were obtained using a Perkin Elmer Simultaneous Thermal Analyzer (STA) 6000 and analyzed using Pyris Series data software. Open ceramic pans were employed here with an empty pan serving as reference. The DSC and TG experiments were carried out under

high purity inert nitrogen gas atmosphere. Samples were heated at 10 °C·min^{-1} from approximately 45 °C to 260 °C.

2.2 General methods for the synthesis of OED and SED

A standard Grignard addition reaction of cyclohexylmagnesium bromide was performed on the xanthone **1** (Scheme 2), in anhydrous THF, to afford the respective alcohol **2** in moderate to good yields. To the alcohol, dissolved in a mixture of acetic anhydride and dichloromethane and cooled in an ice/water bath, was added perchloric acid dropwise. Diethyl ether was then added to the solution in order to ensure crystallization of the perchlorate salt **3**, which was filtered and washed with diethyl ether, and dried overnight under high vacuum. Afterwards, the perchlorate salt was dissolved in dichloromethane, and ethylenediamine was added dropwise. The resulting solution was stirred overnight and then washed with water (3 x 300 mL). The organic layer was separated and dried over sodium sulfate, and the dichloromethane removed using a rotary evaporator. The resulting gum was crystallized using dichloromethane and petroleum ether (bp 40–60 °C) to afford the host material, OED or SED, as applicable, which was dried under high vacuum before it was used in subsequent host-guest experiments.
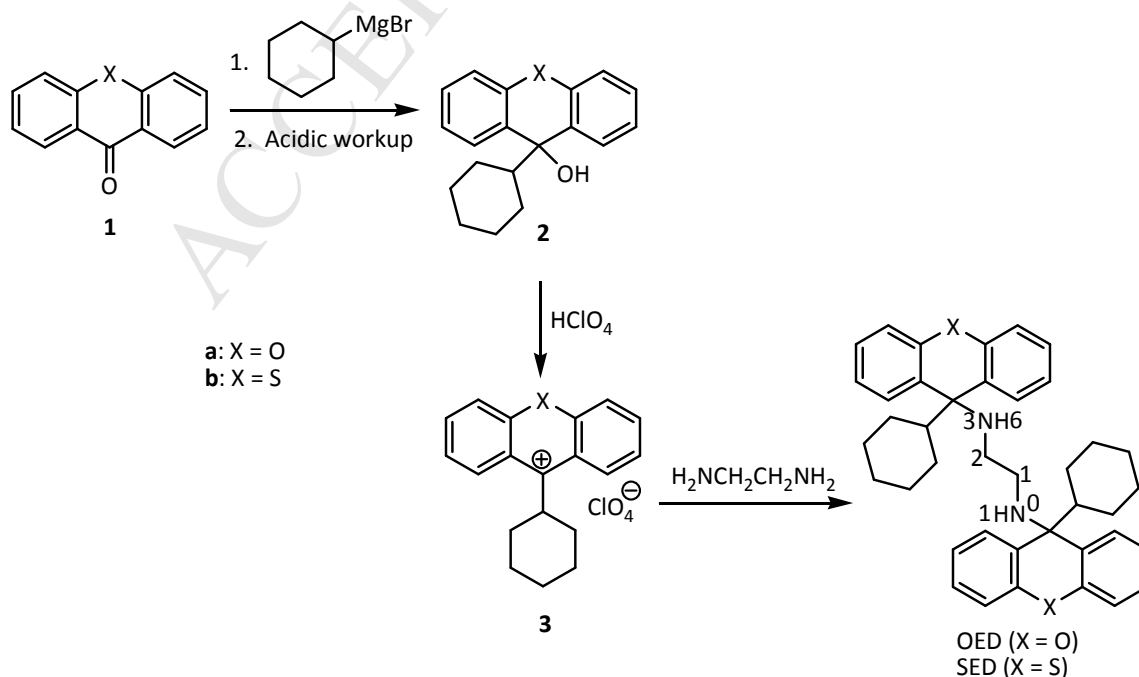
Scheme 2. Synthetic strategy towards compounds OED and SED

2.2.1 Synthesis of OED

2.2.1.1   9-Cyclohexylxanthen-9-ol (2a).   Magnesium turnings (3.52 g, 144.8 mmol), bromocyclohexane (23.30 g, 142.9 mmol) and xanthone (13.90 g, 70.8 mmol) yielded 9-cyclohexylxanthen-9-ol (2a) (8.66 g, 30.9 mmol, 43.6%) as a white solid, mp 160–162 °C; v_{max}(solid)/cm^{-1} 3394 (OH), 2930 (CH), 2852 (CH), 1600 (Ar) and 1572 (Ar); δ_H(CDCl$_3$)/ppm 0.69–1.16 (5H, m, 2C$\underline{H}_2$CH and C$\underline{H}$COH), 1.46–1.76 (6H, m, 3C$\underline{H}_2$CH$_2$), 2.28 (1H, s, CHCO$\underline{H}$), 7.12–7.41 (6H, m, Ar$\underline{H}$) and 7.68 (2H, d, Ar$\underline{H}$); δ_C(CDCl$_3$)/ppm 26.21 ($\underline{C}$H$_2$CH), 26.25 ($\underline{C}$H$_2$CH$_2$), 26.82 ($\underline{C}$H$_2$CH$_2$), 52.68 ($\underline{C}$HCOH), 71.87 ($\underline{C}$OH), 115.74 (Ar$\underline{C}$), 122.96 (Ar$\underline{C}$), 126.91 (Ar$\underline{C}$), 127.12 (quaternary Ar$\underline{C}$), 128.52 (Ar$\underline{C}$) and 151.03 (quaternary Ar$\underline{C}$) (see Figure S1 in the Supplementary Information).

2.2.1.2 9-Cyclohexyl-9-xanthenylium perchlorate (3a). 9-Cyclohexylxanthen-9-ol (5.02 g, 17.9 mmol), perchloric acid (1.40 mL), acetic anhydride (5 mL) and diethyl ether (30 mL) afforded 9-cyclohexyl-9-xanthenylium perchlorate (3a) (6.05 g, 16.7 mmol, 92.7%) as a bright orange solid, mp 179–182 °C; v_{max}(solid)/cm^{-1} 2937 (CH), 2865 (CH) and 1620 (Ar); δ_H(CDCl$_3$)/ppm 1.84–2.64 (10H, m, 5C$\underline{H}_2$), 4.36 (1H, t, C$\underline{H}$-C$^+$), 8.06–8.11 (2H, m, Ar), 8.34–8.36 (2H, m, Ar), 8.47–8.49 (2H, m, Ar), 8.98–9.00 (2H, m, Ar); δ_C(CDCl$_3$)/ppm 18.38 ($\underline{C}$H$_2$CH), 26.53 ($\underline{C}$H$_2$CH$_2$), 28.46 ($\underline{C}$H$_2$CH$_2$), 31.22 ($\underline{C}$HC$^+$), 58.54 (CH$\underline{C}^+$), 116.35 (Ar$\underline{C}$), 122.46 (Ar$\underline{C}$), 126.82 (quaternary Ar$\underline{C}$), 127.03 (Ar$\underline{C}$), 128.07 (Ar$\underline{C}$) and 154.85 (quaternary ArC) (see Figure S2 in the Supplementary Information).

2.2.1.3   *N,N'*-Bis(9-cyclohexyl-9-xanthenyl)ethylenediamine   (OED).   9-Cyclohexyl-9-xanthenylium perchlorate (5.09 g, 14.03 mmol) and ethylenediamine (1.16 g, 19.3 mmol) afforded *N,N'*-bis(9-cyclohexyl-9-xanthenyl)ethylenediamine (OED) (3.82 g, 6.53 mmol, 46.5%)

as a white solid, mp 209–211 °C; v_{max}(solid)/cm^{-1} 2926 (CH), 2852 (CH), 1598 (Ar) and 1573 (Ar); δ_H(CDCl$_3$)/ppm 0.76–1.14 (10H, m, 4C$\underline{H}_2$CH and 2C$\underline{H}$CNH), 1.56–1.70 (12H, m, 6C$\underline{H}_2$CH$_2$), 2.15–2.25 (6H, m, 2N$\underline{H}$C$\underline{H}_2$) and 7.12–7.50 (16H, m, Ar$\underline{H}$); δ_C(CDCl$_3$)/ppm 26.40 ($\underline{C}$H$_2$CH), 26.83 ($\underline{C}$H$_2$CH$_2$), 27.31 ($\underline{C}$H$_2$CH$_2$), 44.05 (NH$\underline{C}$H$_2$), 54.31 ($\underline{C}$HCNH), 60.52 (CH$\underline{C}$NH), 115.99 (Ar$\underline{C}$), 122.52 (Ar$\underline{C}$), 124.41 (Ar$\underline{C}$), 127.56 (Ar$\underline{C}$), 127.80 (quaternary Ar$\underline{C}$) and 152.72 (quaternary Ar$\underline{C}$). (Found for C$_{40}$H$_{44}$O$_2$N$_2$: 82.04% C, 7.75% H, 4.71% N. Calculated 82.15% C, 7.58% H, 4.79% N) (see Figure S3 in the Supplementary Information).

2.2.2 Synthesis of SED

2.2.2.1 9-Cyclohexylthioxanthen-9-ol (2b). Magnesium turnings (3.44 g, 141.5 mmol), bromocyclohexane (23.04 g, 141.3 mmol) and thioxanthone (15.04 g, 70.9 mmol) yielded 9-cyclohexylthioxanthen-9-ol (2b) (7.75 g, 26.1 mmol, 37.0%) as a light cream solid, mp 144–146 °C; v_{max}(solid)/cm^{-1} 3445 (OH), 2929 (CH), 2850 (CH), 1583 (Ar) and 1561 (Ar); δ_H(CDCl$_3$)/ppm 1.03–1.64 (10H, m, 3C$\underline{H}_2$CH$_2$ and 2C$\underline{H}_2$CH), 2.02 (1H, t, C$\underline{H}$COH), 2.25 (1H, s, CHCO$\underline{H}$), 7.26–7.44 (6H, m, Ar$\underline{H}$) and 7.78–7.79 (2H, m, Ar$\underline{H}$); δ_C(CDCl$_3$)/ppm 26.29 ($\underline{C}$H$_2$CH), 26.47 ($\underline{C}$H$_2$CH$_2$), 26.70 ($\underline{C}$H$_2$CH$_2$), 40.90 ($\underline{C}$HCOH), 77.75 (CH$\underline{C}$OH), 125.84 (Ar$\underline{C}$), 126.48 (Ar$\underline{C}$), 126.59 (Ar$\underline{C}$), 126.85 (Ar$\underline{C}$), 130.39 (quaternary Ar$\underline{C}$) and 139.75 (quaternary Ar$\underline{C}$) (see Figure S4 in the Supplementary Information).

2.2.2.2 9-Cyclohexyl-9-thioxanthenylium perchlorate (3b). 9-Cyclohexylthioxanthen-9-ol (5.01 g, 16.9 mmol), perchloric acid (1.50 ml), acetic anhydride (5 mL) and diethyl ether (35 mL) afforded 9-cyclohexyl-9-thioxanthenylium perchlorate (3b) (5.50 g, 14.5 mmol, 86.1%) as a crimson red solid, mp 124–126 °C; v_{max}(solid)/cm^{-1} 2915 (CH), 2857 (CH) and 1628 (Ar); δ_H(CDCl$_3$)/ppm 2.04–2.63 (10H, m, 5C$\underline{H}_2$), 4.49 (1H, t, C$\underline{H}$-C$^+$), 8.17–8.33 (4H, m, Ar$\underline{H}$), 8.64–8.72 (2H, m, Ar$\underline{H}$) and 9.22–9.24 (2H, d, Ar$\underline{H}$). [This perchlorate was unstable in the atmosphere and converted back to the alcohol form (9-cyclohexylthioxanthen-9-ol). Therefore, resonance peaks in the ^{13}C-NMR spectrum could not be confidently assigned. (See Figure S5 in the Supplementary Information).]

2.2.2.3 **_N,N'_-Bis(9-cyclohexyl-9-thioxanthenyl)ethylenediamine (SED).** 9-Cyclohexyl-9-thioxanthenylium perchlorate (5.01 g, 13.2 mmol) and ethylenediamine (1.08 g, 18.0 mmol) afforded _N,N'_-bis(9-cyclohexyl-9-thioxanthenyl)ethylenediamine (SED) (2.70 g, 4.38 mmol, 33.2%) as a white solid, mp 238–240 °C; v_{max}(solid)/cm^{-1} 2919 (CH), 2848 (CH), 1584 (Ar) and 1558 (Ar); δ_H(CDCl$_3$)/ppm 1.02 (10H, m, 4C$\underline{H}_2$CH and 2C$\underline{H}$CNH), 1.57–1.74 (12H, m, 6C$\underline{H}_2$CH$_2$), 2.20 (2H, s, 2N$\underline{H}$CH$_2$), 2.44 (4H, s, 2NHC$\underline{H}_2$), 7.25–7.33 (12H, m, Ar$\underline{H}$) and 7.68–7.69 (4H, m Ar$\underline{H}$); δ_C(CDCl$_3$)/ppm 26.51 ($\underline{C}$H$_2$CH$_2$), 26.81 ($\underline{C}$H$_2$CH$_2$), 27.21 ($\underline{C}$H$_2$CH), 43.75 ($\underline{C}$HCNH), 50.15 (NH$\underline{C}$H$_2$), 65.77 (CH$\underline{C}$NH), 125.20 (Ar$\underline{C}$), 125.82 (Ar$\underline{C}$), 126.58 (Ar$\underline{C}$), 129.41 (Ar$\underline{C}$), 131.96 (quaternary Ar$\underline{C}$) and 135.64 (quaternary Ar$\underline{C}$). (Found for C$_{40}$H$_{44}$S$_2$N$_2$: 77.60% C, 7.08% H, 4.48% N, 10.11% S. Calculated 77.88% C, 7.19% H, 4.54% N, 10.39% S) (See Figure S6 in the Supplementary Information).

2.3 Single solvent experiments

The single solvent experiments were conducted in glass vials. Hosts OED (0.050 g, 0.085 mmol) or SED (0.050 g, 0.081 mmol) were independently dissolved in an excess of each of the potential guest compounds (5 mmol). These mixtures were gently heated using a hot water bath, if necessary, to ensure dissolution of all of the host material. The vials were then left open at room temperature and at ambient pressure until crystallization occurred. The crystals were collected using vacuum filtration, washed with petroleum ether (bp 40–60 °C) and analysed by means of ^{1}H-NMR spectroscopy, with CDCl$_3$ as the solvent, in order to determine if inclusion had occurred. When complexation was successful, the host:guest (H:G) ratios were determined through integration of relevant host and guest resonance signals.

2.4 Competition experiments

2.4.1   Equimolar guest mixtures.   Competition experiments were carried out in order to determine whether hosts OED and SED possessed the ability to discriminate between the various guests when presented with a guest mixture.   The hosts were thus individually recrystallized, in glass vials, from equimolar binary, ternary and quaternary mixtures of the xylenes and EB.   The vials were closed and stored in a refrigerator at 0 °C.   Crystals that formed were treated in the same way as previously mentioned.   The guest:guest (G:G) ratios of the inclusion complexes were determined using GC-MS, and the overall H:G ratio by means of ^{1}H-NMR spectroscopy.

2.4.2   Non-equimolar guest mixtures.   The host was independently recrystallized from various binary combinations of the four guest solvents, but the concentrations of these guests were now varied.   The G1:G2 mixtures that were employed varied from molar ratios of 20:80 to 80:20.   The vials were treated in the same manner as for the equimolar experiments before, and the mother liquors as well as the crystals that formed from these mixtures were analysed using GC-MS.   The molar fraction of guest in the crystals (Y) was plotted against the molar fraction of the same guest in the mother liquor (X) to obtain the selectivity profiles provided in Figure 1.

2.5 Computational methods

Using Spartan '10 V1.1.0,[27] supplied by Wavefunction Inc., computational methods were carried out on both OED and SED.   A conformational search was thus conducted on each host compound on the molecular mechanics level using the Monte-Carlo algorithm and MMFF force field.   Both hosts yielded 100 conformers of which only the three lowest energy conformers (OED*a–c* and SEDa–c, in ascending energy order) were used in subsequent calculations with ground state energetics at the DFT (density functional theory) BLYP/6-31G* through to the higher DFT B3LYP/6-311G* levels.

3. Results and discussion

Hosts compounds OED and SED were readily prepared by reacting the xanthone **1** with the Grignard reagent cyclohexylmagnesium bromide (Scheme 2). After work-up, the resulting alcohols **2** were treated with perchloric acid to yield salts **3**, which were then linked by means of a reaction with ethylenediamine to afford the title host compounds, OED and SED, in low to moderate yields.

3.1 Single solvent experiments

Table 1 contains data obtained after recrystallization of OED and SED from each of *o*-Xy, *m*-Xy, *p*-Xy and EB, and analysis of the resulting crystals by means of ^{1}H-NMR spectroscopy.

Table 1

H:G ratios^a for the single solvent experiments using OED and SED

Host	Guest	H:G ratio^a
OED	*o*-Xy	2:1
OED	*m*-Xy	^{b}
OED	*p*-Xy	2:1
OED	EB	2:1
SED	*o*-Xy	^{b}
SED	*m*-Xy	^{b}
SED	*p*-Xy	^{b}
SED	EB	^{b}

^{a}Determined using ^{1}H-NMR spectroscopy, with CDCl$_3$ as the deuterated solvent
^{b}No inclusion occurred

Surprisingly, OED and SED displayed significantly different host ability in the presence of the C8 aromatics. While OED was efficient, clathrating all (with 2:1 H:G ratios) but the *m*-Xy isomer, SED failed to form complexes with any of these solvents (Table 1). We also investigated whether it would be possible to encourage SED to enclathrate *p*-Xy by preparing a nearly saturated solution of SED in *p*-Xy, carefully filtering this solution, and seeding it with crystals of the complex OED·*p*-Xy. The crystals that so-formed were analysed by means of ^{1}H-NMR

spectroscopy (see Supplementary Information, Figure S7) which showed that only apohost SED crystallized out and, hence, *p*-Xy remained uncomplexed despite the presence of the OED·*p*-Xy complex.

We consequently investigated the selectivity behaviour of OED and SED when presented with various mixtures of these guests.

3.2 Competition experiments

3.2.1 Equimolar guest mixtures. Unsurprisingly, owing to the lack of host ability observed in the single solvent experiments, SED failed to form any complexes, mixed or otherwise, when presented with the guest mixtures. As expected, however, OED remained efficient in these conditions, and formed mixed complexes in most of these experiments when recrystallized from the equimolar binary, ternary and quaternary guest mixtures. Table 2 summarises the data obtained (for OED), where preferred guests are highlighted in red.

Table 2

Competition experiment results for OED when recrystallized from equimolar mixtures of *o*-Xy, *m*-Xy, *p*-Xy and EB[a]

o-Xy	*m*-Xy	*p*-Xy	EB	Guest ratios (% e.s.d.s)[b]	Overall H:G ratio
X	X			**81.2**:18.8 (0.4)	2:1
X		X		**64.9**:35.1 (0.2)	2:1
X			X	c	c
	X	X		c	c
	X		X	c	c
		X	X	**58.5**:41.5 (0.2)	2:1
X	X	X		**59.3**:10.6:30.1 (1.6)(0.6)(1.0)	2:1
X	X		X	**66.2**:10.9:22.9 (1.6)(0.9)(0.7)	2:1
X		X	X	**53.4**:27.6:19.0 (1.4)(0.6)(0.8)	2:1

	X	**X**	X	16.5:**48.3**:35.2 (0.5)(0.0)(0.5)	2:1
X	X	X	X	**49.2**:8.1:24.8:17.9 (1.5)(0.2)(0.4)(0.9)	2:1

[a]GC-MS and ^{1}H-NMR spectroscopy were used to obtain the guest and overall H:G ratios, respectively
[b]The competition experiments were conducted in triplicate; % estimated standard deviations (% e.s.d.s) are provided in parentheses
[c]No inclusion occurred

For each binary competition experiment in which *o*-Xy was present (*o*-XyXy/*m*-Xy and *o*-Xy/*p*-Xy), with the exception of *o*-Xy/EB, this was the preferred guest (81.2% and 64.9%, respectively) (Table 2). The *o*-Xy/EB experiment afforded crystals, but no guest was included. OED, furthermore, displayed a slight affinity for *p*-Xy (58.5%) when it was recrystallized from a *p*-Xy/EB solution. Mixtures comprising *m*-Xy/*p*-Xy and *m*-Xy/EB also yielded no complexes in these experiments.

Competition experiments involving ternary guest mixtures (*o*-Xy/*m*-Xy/*p*-Xy, *o*-Xy/*m*-Xy/EB and *o*-Xy/*p*-Xy/EB) all showed that *o*-Xy remained preferred (59.3%, 66.2% and 53.4%, respectively), as was the case in the binary experiments. The ternary equimolar *m*-Xy/*p*-Xy/EB competition experiment, in the absence of *o*-Xy, permitted *p*-Xy (48.3%) to now be preferred followed by 35.2% EB and 16.5% *m*-Xy. Therefore, results from these ternary equimolar experiments suggested a host selectivity order of *o*-Xy > *p*-Xy > EB > *m*-Xy, which was in agreement with the quaternary competition experiment that was conducted (49.2% *o*-Xy >24.8% *p*-Xy > 17.9% EB > 8.1% *m*-Xy).

The preference of OED for the *ortho* isomer is unprecedented in our laboratories, and (*R*,*R*)-(−)-2,3-dimethoxy-1,1,4,4-tetraphenylbutane-1,4-diol,[19] *N*,*N'*-bis(9-phenyl-9-thioxanthenyl)ethylenediamine,[20] *trans*-*N*,*N'*-bis(9-phenyl-9-xanthenyl)cyclohexane-1,4-diamine and *trans*-*N*,*N'*-bis(9-phenyl-9-thioxanthenyl)cyclohexane-1,4-diamine[21] always favoured *p*-Xy when these guests competed.

3.2.2 Non-equimolar guest mixtures. OED was recrystallized from binary guest mixtures in which the concentration of the constituent guests were varied in order to observe whether the selectivity of the host, obtained from the equimolar experiments, is affected in such changing conditions. Thus Figures 1a–c represent the selectivity profiles obtained for the *o*-Xy/*m*-Xy, *o*-Xy/*p*-Xy and *p*-Xy/EB experiments; *o*-Xy/EB, *m*-Xy/EB and *m*-Xy/*p*-Xy mixtures were not considered here since these furnished no complexes in the equimolar experiments. Note that the line that represents an unselective host is denoted by the black dotted line in each figure.
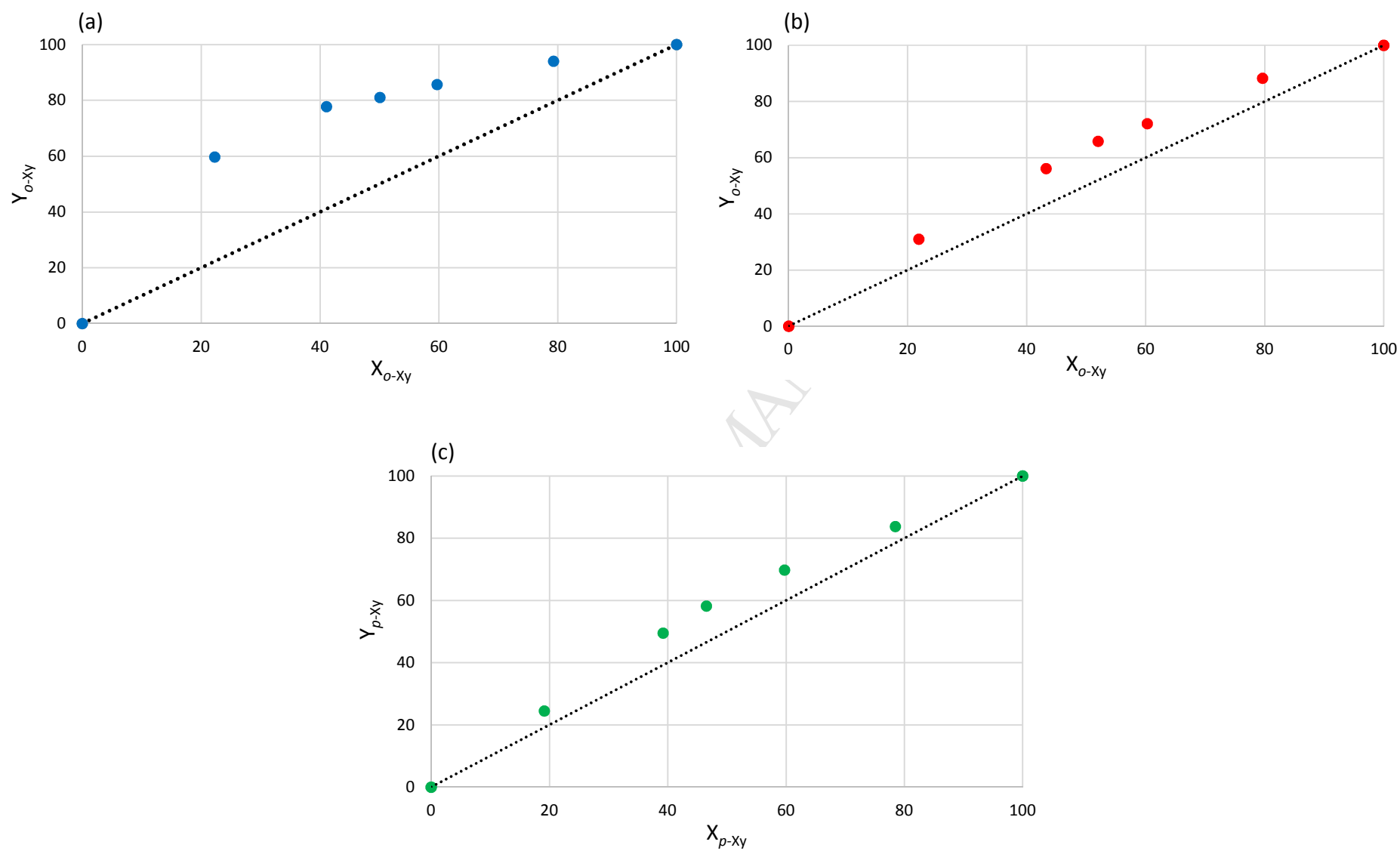
Figure 1. Selectivity profiles for the (a) o-Xy/m-Xy, (b) o-Xy/p-Xy and (c) p-Xy/EB competition experiments

Figure 1a displays the selectivity profile for OED when recrystallized from various *o*-Xy/*m*-Xy mixtures. *o*-Xy was significantly favoured over *m*-Xy over the entire concentration range. At 22.3% *o*-Xy in the mother liquor, OED already contained 59.6% of this guest. The selectivity for *o*-Xy persisted as the concentration of this guest in the mother liquor increased further, and the complex that resulted when 79.3% *o*-Xy was present in the mother liquor contained 94.0% *o*-Xy. The binary *o*-Xy/*p*-Xy competition experiment resulted in the selectivity profile that is provided in Figure 1b. At a low concentration of *o*-Xy (21.9%) in this solution, this guest was preferred by OED, and 31.0% *o*-Xy was present in the resultant complex. However, as the concentration of *o*-Xy was increased, only subtle changes in the selectivity for *o*-Xy was observed: a complex containing 88.3% of this guest was obtained when the mother liquor contained 79.6% *o*-Xy. In the *p*Xy/EB experiment (Figure 1c), the host displayed only a slight preference for the *p*-Xy guest relative to EB. The selectivity for *p*-Xy was 24.5% when the solution contained 19.2% *p*-Xy, while a 78.5% *p*-Xy mixture resulted in a complex containing 83.8% *p*-Xy.

While the selectivity of OED for *o*-Xy in all applicable competition experiments may only be described as adequate, what is striking is the vast differences in behaviour between OED and SED despite the only variance being in their B rings. In order to better understand why these compounds behave so differently, we conducted an in-depth analysis of their conformations by means of computational calculations, and compared these results with the crystal structures of apohosts OED and SED.

3.3 Computational methods

Both OED and SED displayed similar calculated geometries for the three lowest energy conformers OED*a–c* and SED*a–c*. (The atomic coordinates of the calculated structures have been deposited in the Supplementary Information.) The two lowest energy conformers *a* and *b* had their the nitrogen atoms in a *gauche* conformation when observing along the C_1–C_2 bond of the ethylenediamine linker (Figures 2.1a and 2.2a, and 2.1b and 2.2b, respectively) (see Scheme

2 for atomic labelling) while, in the instance of the third lowest energy conformer *c*, the nitrogen atoms were arranged in an *anti*-orientation relative to this C_1–C_2 bond (Figures 2.1c and 2.2c). This energy order of the conformers *a–c* at the higher computational levels was maintained, with the exception that at the BLYP/6-31+G* level for the geometry of host SED, conformers *b* and *c* were reversed energetically. These energies together with $N_0 \cdots N_3$ and $H_1 \cdots N_3$ distances, and N_0–C_1–C_2–N_3 ($N_0 \cdots N_3$) dihedral angles, are provided in Table 3.

Table 3

Calculated energies, distances and relevant angles for the OED*a–c* and SED*a–c* conformers

Computational level	Conformer	Energy (kJ·mol^{-1})	Relative Energy (kJ·mol^{-1})	Dihedral angle N_0–C_1–C_2–N_3 (°)	Distance N_0···N_3 (Å)	Distance H_1···N_3 (Å)
DFT (BLYP/6-31G*)	OED*a*	−4751758.33	0	−62.29		
	OED*b*	−4751754.25	4.09	−59.38		
	OED*c*	−4751752.78	5.56	180		
	SED*a*	−6447579.49	0	62.01		
	SED*b*	−6447576.01	3.48	−67.75		
	SED*c*	−6447574.06	5.42	180		
DFT (BLYP/6-31+G*)	OED*a*	−4751920.10	0	−66.75	3.008	3.425
	OED*b*	−4751919.00	1.1	−62.48	2.956	2.544
	OED*c*	−4751918.30	1.8	180	3.774	4.064
	SED*a*	−6447730.79	0	64.11	2.973	
	SED*b*	−6447728.45	2.34	−63.96	2.973	
	SED*c*	−6447728.63	2.16	180	3.771	
DFT (B3LYP/6-31G**)	OED*a*	−4754236.04	0	−62.4	2.905	3.263
	OED*b*	−4754231.53	4.51	−58.95	2.863	2.428
	OED*c*	−4754229.92	6.12	180	3.733	4.026
	SED*a*	−6450112.37	0	60.32	2.888	
	SED*b*	−6450108.88	3.49	−61.42	2.903	
	SED*c*	−6450107.20	5.17	180	3.732	
DFT (B3LYP/6-311G*)	OED*a*	−4755040.93	0	−64.3	2.943	3.356
	OED*b*	−4755039.21	1.71	−60.84	2.897	2.484
	OED*c*	−4755038.05	2.88	180	3.733	4.029
	SED*a*	−6450940.77	0	60.9	2.903	
	SED*b*	−6450937.97	2.8	−62.3	2.922	
	SED*c*	−6450936.64	4.14	180	3.732	

The $N_0 \cdots N_3$ dihedral angles of the computed conformers of OED ranged between −62.29 and −66.75° for *a*, −58.95 and −62.48° for *b*, and 180° for *c* (Table 3). In SED, these angles ranged from 60.32 to 64.11° (*a*), −61.42 to −67.75° (*b*) and 180° (*c*). It is therefore evident that the two nitrogen atoms of the *a* conformers in each host are situated in the *gauche* orientation but these are on opposite sides of the C_1–C_2 bond. For conformers *b* and *c* for both hosts, on the other hand, these angles are comparable. In the structures of conformers OED*a–c* and SED*a–c*, after the final DFT level calculation (Figures 2.1a–c and 2.2a–c), the shape of the ethylenediamine linker (N_0–C_1–C_2–N_3) in conformers *a* and *b* is bucket-like, whereas this linker of the *c* conformers of OED and SED exhibits a zig-zagged orientation.

The $N_0 \cdots N_3$ and $H_1 \cdots N_3$ distances were calculated at the DFT (BLYP/6-31+G*) and higher levels for conformers OED*a–c*, while only the former were calculated for conformers SED*a–c* since this host did not experience an intramolecular N_0–$H_1 \cdots N_3$ hydrogen bond in the crystal (discussed later) (Table 3). The $N_0 \cdots N_3$ distances for corresponding conformers for both hosts were similar. For example, this distance for OED*a* ranged between 2.905 and 3.008 Å while, correspondingly, SED*a* ranged from 2.888 and 2.973 Å. The $H_1 \cdots N_3$ distances of conformers *a–c* of host SED differed extensively, as expected, with the *anti* conformer *c* having the longest of these (4.026–4.064 Å) and which, as a result of the orientations of the nitrogen groups, are not able to hydrogen bond. Interestingly, conformer OED*b* experienced the shortest hydrogen bond ($H_1 \cdots N_3$ 2.428–2.544 Å) compared with conformers *a* (3.263–3.425 Å) and *c* (4.026–4.064 Å).

The electrostatic potential maps for conformers OED*a–c* and SED*a–c*, after the DFT B3LYP/6-311G* level calculation, are provided in Figures 2.1a–c and 2.2a–c, respectively. Electron-rich areas are red while the dark blue regions indicate electron-poor regions. The oxygen and sulfur atoms are shown in red and yellow, respectively.
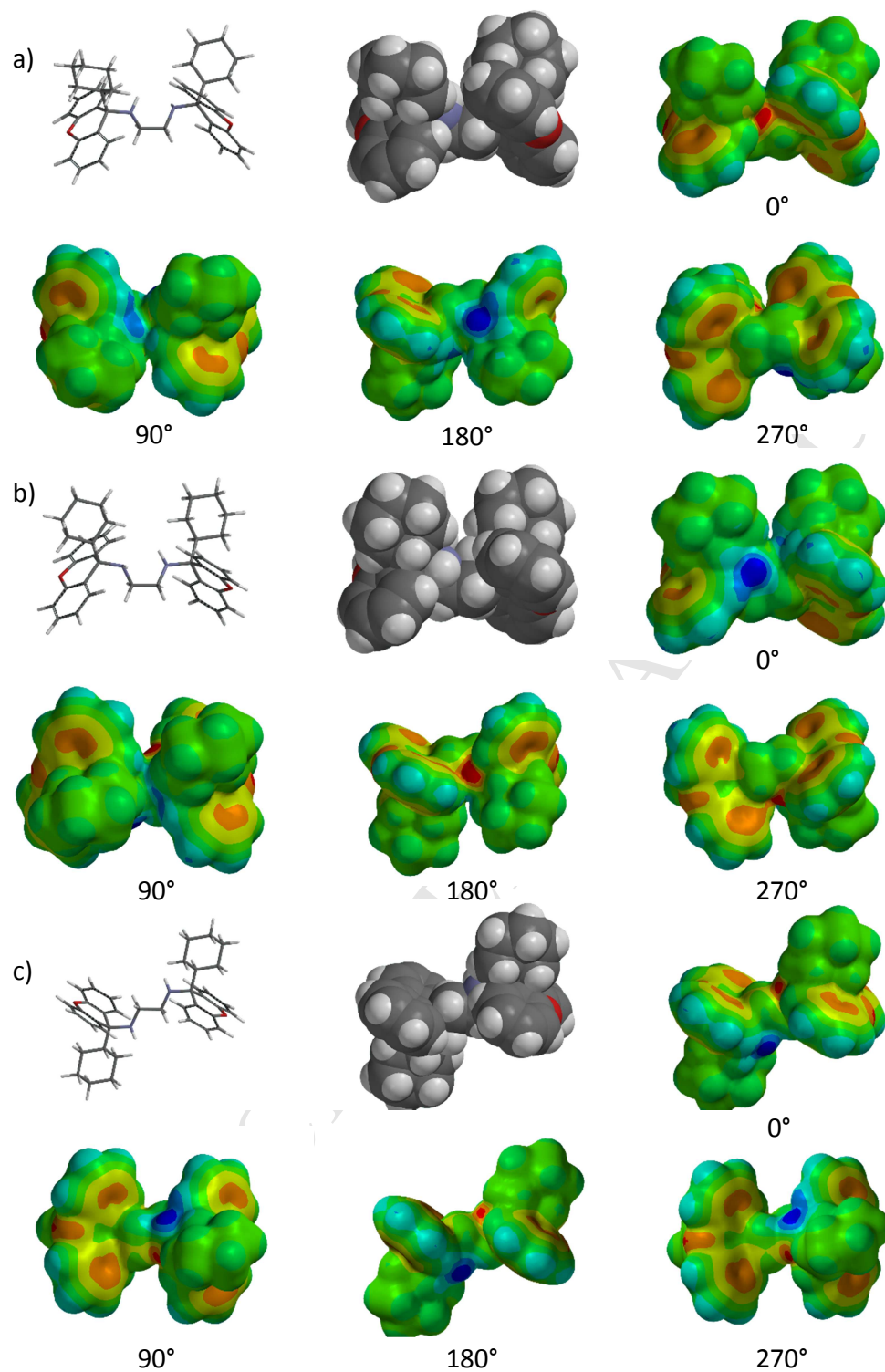
a)

0°

90°   180°   270°

b)

0°

90°   180°   270°

c)

0°

90°   180°   270°

Figure 2.1 The structures of the computed OED*a–c* conformers, displayed in tube form and spacefill representations, and their electrostatic potential maps at 90° rotation intervals
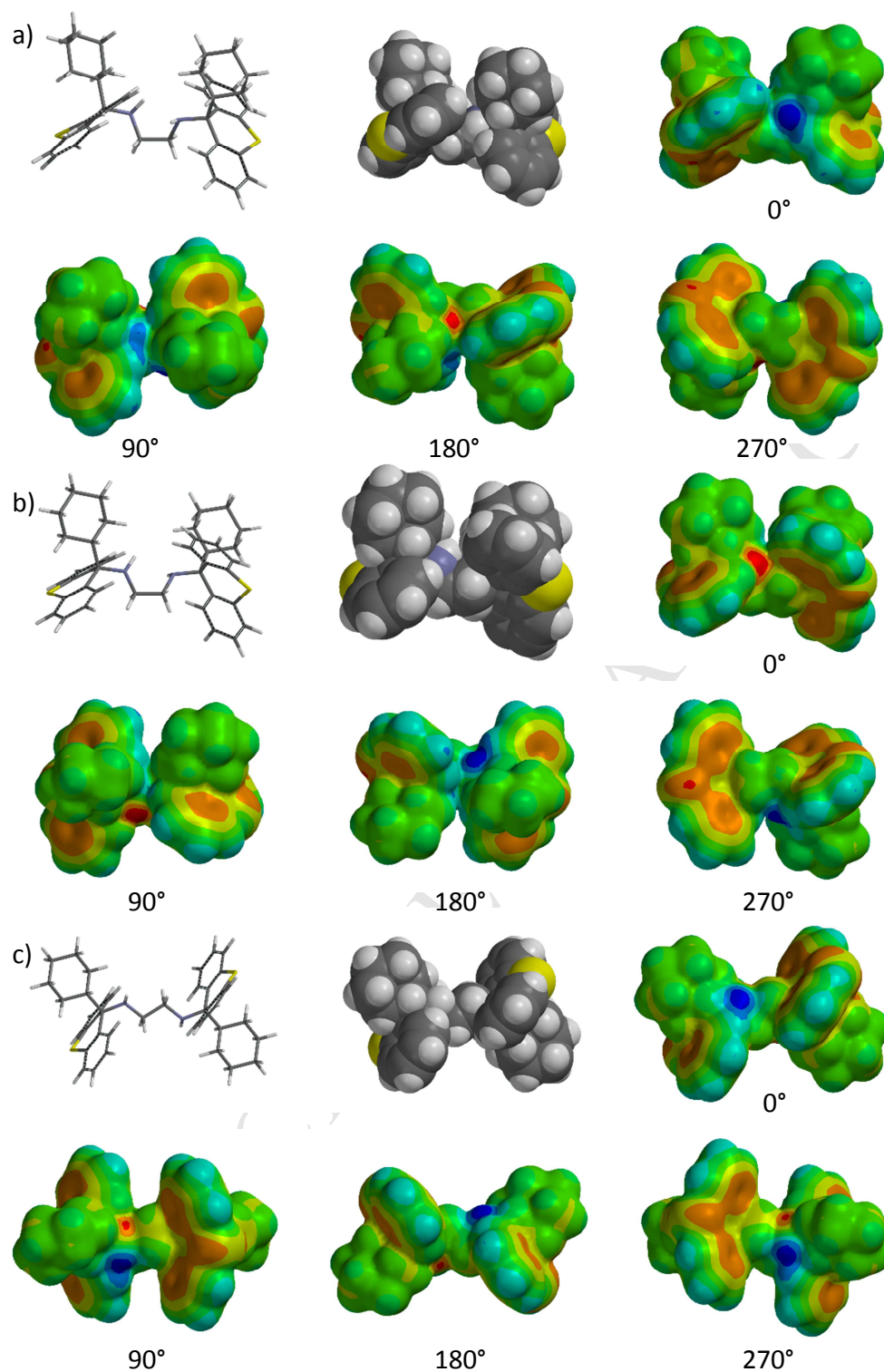
Figure 2.2 The structures of conformers SED*a–c*, displayed in a tube and spacefill form, accompanied by their electrostatic potential maps which are displayed at 90° rotation intervals

We subsequently investigated the geometries of OED and SED in their pure crystal forms by means of SCXRD experiments for comparison purposes with these calculated geometries.

3.4 SCXRD analyses of apohosts OED and SED

SCXRD analyses were conducted on suitable crystals of the pure hosts OED and SED when they were recrystallized from *m*-xylene and 2-methylpyridine, respectively (these solvents were not enclathrated in this way). The crystallographic data and refinement parameters for both compounds are provided in Table 4. Both crystallized in the triclinic crystal system and *P*-1 space group but the host packing differed in each. Furthermore, both hosts displayed disorder of the nitrogen hydrogens over two positions, but only one of the two molecules in the unit cell of SED displayed this type of disorder. Unit cells and host packing diagrams are provided in Figures 3 and 4.

A summary of the non-covalent interactions that hosts OED and SED experience in their crystal structures are provided in Table 5. Interestingly, SED experienced shorter π···π interactions than OED [3.988(1)–5.307(1) Å vs 4.858(1)–5.878(1) Å]. Intermolecular C–H···π interactions were also observed in both structures, and OED was involved in three of these and SED in only one (2.71–2.87 Å, 148–161° and 2.82 Å, 174°, respectively). Only host OED experienced an intramolecular N–H···N bond [2.909(2) Å, 104.8(2)°].

Both hosts displayed intramolecular C–H···N interactions, and these were shorter in SED than OED (2.40–2.53 Å, 102–103° and 2.57–2.61 Å, 102°, respectively). Interestingly, OED was involved in two intermolecular C–H···O–C interactions whereas SED experienced three intermolecular C–H···H–C contacts (2.66–2.69 Å, 133–156° and 2.32–2.36 Å, 121–156°, respectively). All of these interactions assisted in the stabilization of the host packing in the crystals. Furthermore, the distances of the interactions that host SED experienced were considerably shorter than those of OED.

Table 4

	OED	SED
Chemical formula	$C_{40}H_{44}N_2O_2$	$C_{40}H_{44}N_2S_2$
Formula weight	584.77	616.89
Crystal system	triclinic	triclinic
Space group	*P*-1	*P*-1
μ (Mo-Kα)/mm^{-1}	0.073	0.196
a/Å	9.0748(5)	9.5375(3)
b/Å	12.8877(8)	13.0385(4)
c/Å	14.6778(9)	14.7133(5)
alpha/°	94.717(3)	64.928(1)
beta/°	96.443(2)	80.988(1)
gamma/°	106.537(2)	78.669(1)
V/Å^3	1623.43(17)	1619.41(9)
Z	2	2
D(calc)/g.cm^{-3}	1.196	1.265
F(000)	628	660
Temp./K	200	200
Restraints	0	0
Nref	8075	8045
Npar	415	403
R	0.0405	0.0385
wR2	0.1095	0.0970
S	1.02	1.03
θ min–max/°	2.0, 28.4	1.5, 28.4
Tot. data	43830	42664
Unique data	8075	8045
Observed data [I > 2.0 sigma(I)]	6405	6304
R_{int}	0.021	0.026
Completeness	1.000	0.998
Min. resd. dens. (e/Å^3)	−0.22	−0.25
Max. resd. dens. (e/Å^3)	0.31	0.31

Crystallographic data for apohosts OED and SED

(a)

(b)
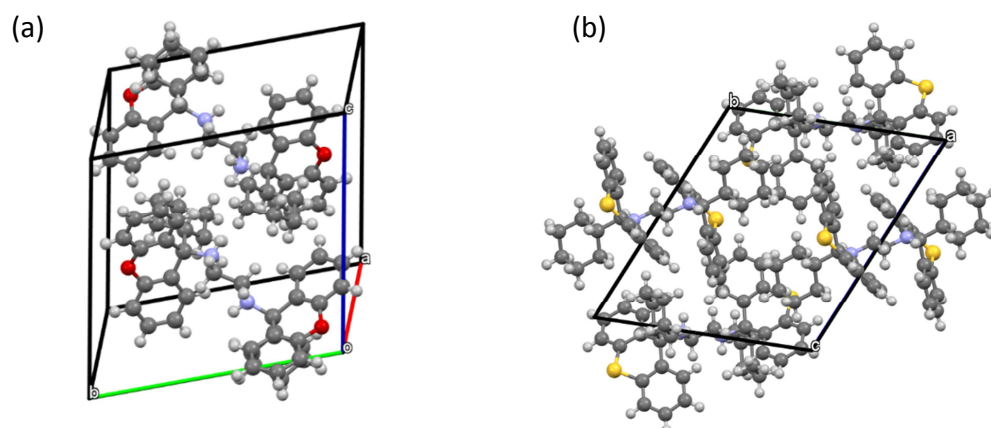
Figure 3. Unit cells of (a) OED and (b) SED

(a)

(b)
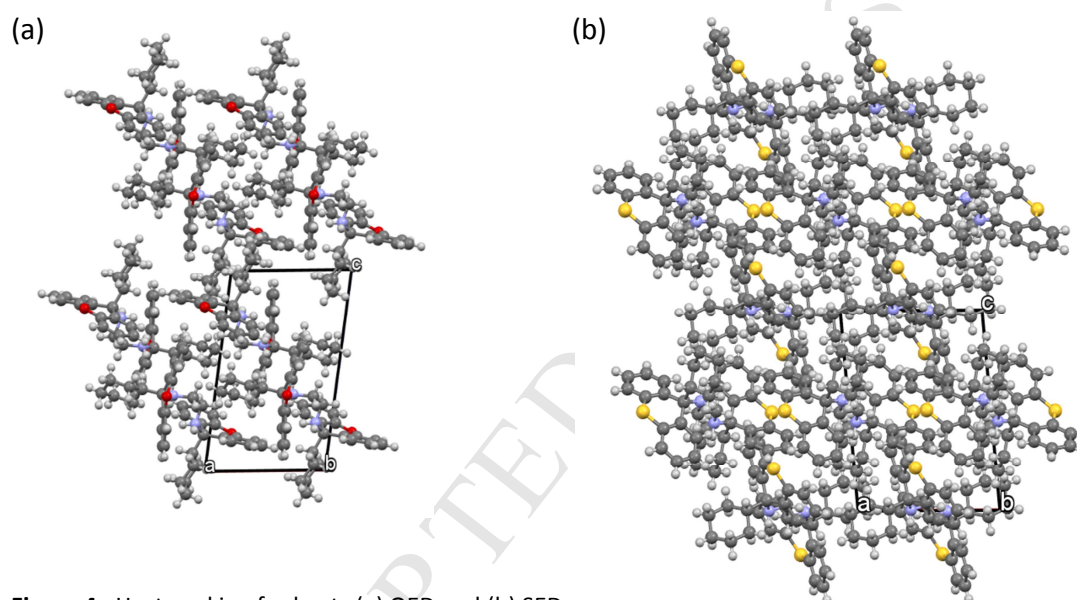
Figure 4. Host packing for hosts (a) OED and (b) SED

Table 5

Interaction	OED	SED	Symmetry
(host)π···π(host)	4.858(1)–5.878(1) Å	3.988(1)–5.307(1) Å	
	(7 contacts)	(6 contacts)	
C–H···π	(H···Cg, X–H···Cg)	(H···Cg, X–H···Cg)	
(host)C–H··· π(host)[c]	2.83 Å, 160°		1–x, 1–y, 1–z
(host)C–H··· π(host)[c]	2.71 Å, 148°		2–x, 1–y, 1–z
(host)C–H··· π(host)[c]	2.87 Å, 161°		–1+x, y, z
(host)C–H··· π(host)[c]		2.82 Å, 174°	x, y, z
Hydrogen bonding			
(host)N–H···N(host)[d]	2.909(2) Å, 104.8(2)°, <<	None	
Other short contacts			
(host)m-ArH···O–C(host)[e]	2.69 Å, 156°, <		2–x, 1–y, 1–z
(host)m-ArH···O–C(host)[e]	2.66 Å, 133°, <		X, 1+y, z
(host)C–H···N(host)[f]	2.61 Å, 102°, <		
(host)C–H···N(host)[f]	2.57 Å, 102°, <		
(host 1)C–H···H–C(host 1)[e]		2.32 Å, 126°, <	–x, 1–y, 2–z
(host 2)m-ArH···H–C(host 1)[e]		2.36 Å, 121°, <	x, y, z
(host 2)C–H···m-ArH(host 1)[e]		2.35 Å, 156°, <	x, 1+y, –1+z
(host 1)o-ArH···N(host 1)[f]		2.40 Å, 103°, <<	
(host 1)o-ArH···N(host 1)[f]		2.53 Å, 102°, <<	
(host 2)o-ArH···N(host 2)[f]		2.47 Å, 102°, <<	
(host 2)o-ArH···N(host 2)[f]		2.46 Å, 103°, <<	

Summary of the non-covalent host···host interactions in the crystals of OED and SED[a,b]

[a]< denotes contacts less than the sum of the van der Waals radii and << contacts less than this sum minus 0.2 Å
[b]One SED host in the crystal contained nitrogen hydrogens that were disordered over two positions; thus the host with no disorder was labelled 'host 1' while the one with disorder was labelled 'host 2'
[c]Intermolecular C–H···π interaction between two host molecules
[d]Intramolecular H–bond within each host molecule
[e]Intermolecular interaction
[f]Intramolecular interaction

Side-to-side, overlaid and stereoviews of the geometries of the calculated conformers that bared a resemblance to that of the geometries of hosts OED and SED in the crystals are provided in Figures 5 and 6, respectively. The calculated conformers have a blue hue in the overlaid view of these structures. Conformer OED*b* closely resembled host OED from the crystal, while conformer SED*c* was similar to that of host SED in the crystal (both conformers were obtained at the DFT B3LYP/6-311G* level).
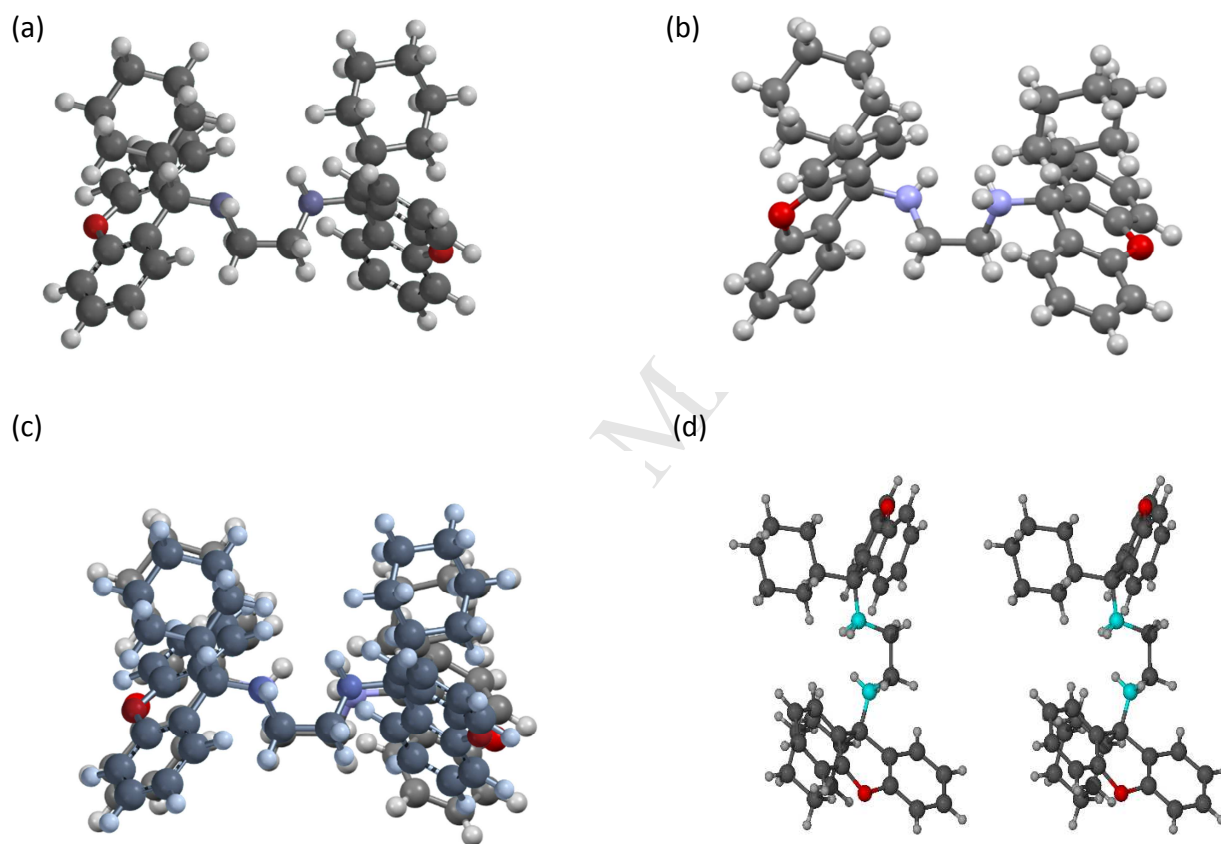
(a)

(b)

(c)

(d)

Figure 5. Geometry of (a) the calculated OED*b* conformer and (b) OED from the crystal; (c) is an overlay of these two (the calculated structure has the blue hue), and (d) a stereoview showing the geometry of each host molecule from the crystal; molecules are shown in ball-and-stick form
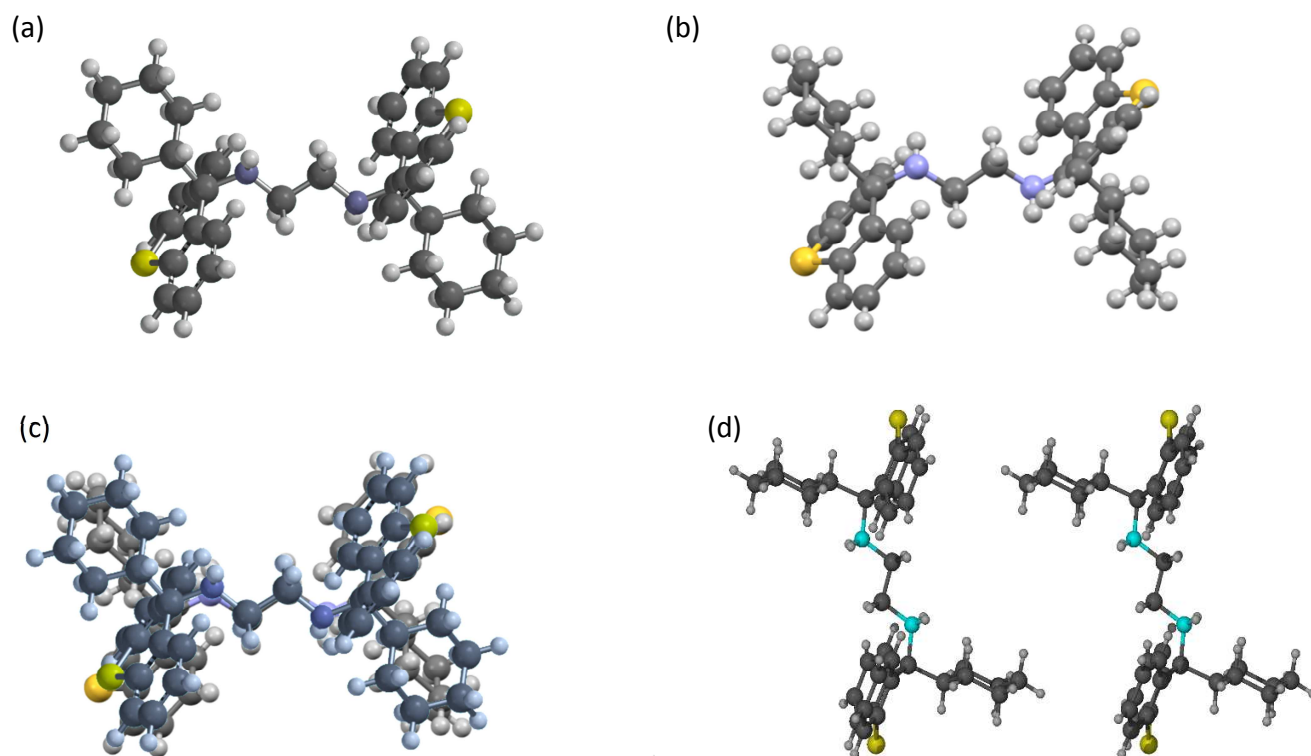
Figure 6. Geometry of (a) the calculated SED*c* conformer and (b) SED from the crystal; (c) is an overlay of these two (the calculated structure, once more, has the blue hue), and (d) a stereoview displaying the molecular geometry of SED from the crystal; molecules are shown in ball-and-stick form

Conformer OED*b* has only a slightly shorter $H_1 \cdots N_3$ bond distance (measured using the Spartan '10 software[27]) compared with OED from the crystal (2.484 and 2.548 Å, respectively). However, this distance in conformers OED*a* and OED*c* is significantly larger than that observed in the crystal (3.356 and 4.029 Å vs 2.548 Å). The SED*c* conformer, on the other hand, had the same N⋯N dihedral angle as SED from the crystal (180°) as well as a comparable distance between the two nitrogen atoms (3.732 and 3.691 Å, respectively). Both host molecules from the crystals therefore occupied higher energy states than conformers *a* (Table 3), but energy differences were small.

This comparative investigation has demonstrated that OED and SED from the crystals possess very different geometries relative to one another, in the orientation of their cyclohexyl and xanthenyl moieties and, most notably, in the geometry of their ethylenediamine linkers. This

observation explains the vastly different host behaviours of the two compounds in the presence of the C8 aromatic fraction. However, an additional experiment was conducted in which a nearly saturated and carefully filtered solution of apohost OED in *m*-Xy (which OED does not clathrate) was seeded with crystals of apohost SED in order to encourage OED to crystallize in the same conformation as SED. However, analysis (SCXRD) of the crystals of OED thus formed revealed, surprisingly, that the conformation of OED was identical to that initially obtained (see Supplementary Information where the .cif file for the obtained structure is provided). Hence this experiment showed that OED could not be encouraged to crystallize in the same conformation as SED despite there being SED crystals present.

3.5 SCXRD analyses of successfully-formed complexes with OED

Table 6 contains the crystallographic data and refinement parameters for the 2OED•*o*-Xy, 2OED•*p*-Xy and 2OED•EB complexes. In all three of these, the guest is disordered around an inversion point, while the nitrogen hydrogens of the host are disordered over two positions, but only in 2OED•EB. All three complexes are isostructural and crystallized in the triclinic crystal system and *P*-1 space group.

Table 6

	2OED•*o*-Xy	2OED•*p*-Xy	2OED•EB
Chemical formula	$C_{40}H_{44}N_2O_2•0.5C_8H_{10}$	$C_{40}H_{44}N_2O_2•0.5C_8H_{10}$	$C_{40}H_{44}N_2O_2•0.5C_8H_{10}$
Formula weight	637.85	637.85	637.85
Crystal system	triclinic	triclinic	triclinic
Space group	*P*-1	*P*-1	*P*-1
μ (Mo-Kα)/mm^{-1}	0.073	0.074	0.074
a/Å	9.4083(3)	9.3877(5)	9.3746(4)
b/Å	13.7868(5)	13.6816(7)	13.7113(6)
c/Å	14.4429(5)	14.4681(7)	14.4735(5)
alpha/°	97.332(2)	97.384(2)	97.950(2)
beta/°	98.449(2)	98.327(2)	98.354(2)
gamma/°	106.820(2)	105.747(2)	105.919(2)
V/Å^3	1744.91(11)	1741.97(16)	1738.76(12)
Z	2	2	2
D(calc)/g.cm^{-3}	1.214	1.216	1.218
F(000)	686	686	686
Temp./K	200	200	200
Restraints	1	0	0
Nref	8708	8690	8670
Npar	467	442	461
R	0.0436	0.0444	0.0435
wR2	0.1172	0.1179	0.1158
S	1.03	1.03	1.05
θ min–max/°	1.9, 28.4	1.9, 28.3	1.9, 28.4
Tot. data	62982	46859	54437
Unique data	8708	8690	8670
Observed data [I > 2.0 sigma(I)]	7165	6656	7115
R_{int}	0.025	0.025	0.025
Completeness	0.999	0.999	0.999
Min. resd. dens. (e/Å^3)	−0.24	−0.24	−0.36
Max. resd. dens. (e/Å^3)	0.34	0.35	0.34

Crystallographic data for 2OED•*o*Xy, 2OED•*p*Xy and 2OED•EB

The unit cell for the 2OED•*p*-Xy complex is provided in Figure 7, as representative example of the three complexes that share the same host packing.
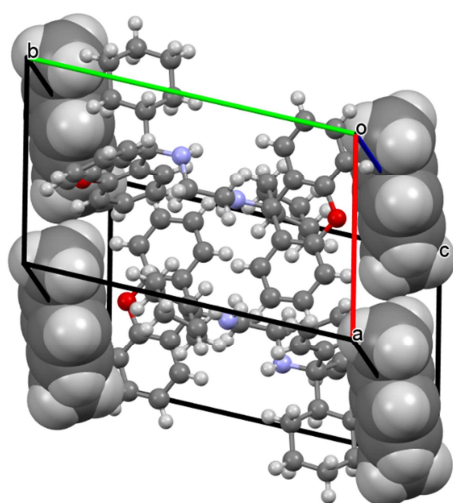
Figure 7. Unit cell of the 2OED•*p*-Xy complex; the host is displayed in ball-and-stick form and the guests in space-fill representation

The guests were removed from the packing calculation and the voids determined using Mercury software.[26] The generation of the voids enlisted the aid of a spherical probe of 1.2 Å that observed the empty spaces in the unit cells that could accommodate this probe. The host–guest packing in the complexes as well as the voids that were thus calculated are shown in Figures 8a and b, respectively (for 2OED•*p*-Xy), and it is clear that the three complexes accommodate their guest molecules in discrete cavities.
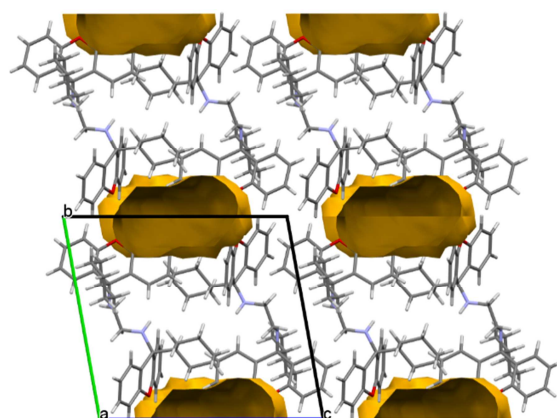
(a)
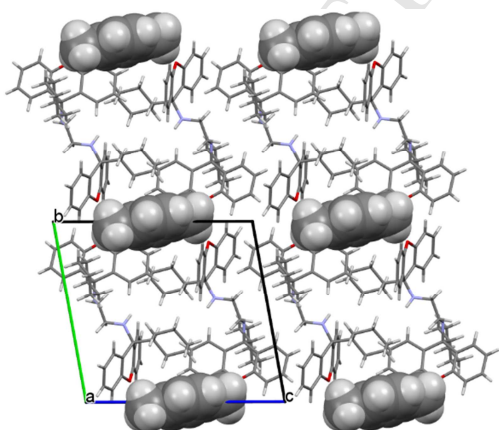
(b)

Figure 8. (a) Host–guest packing in 2OED•-*p*Xy (as representative example); host molecules are presented in capped-stick form and guests in space-fill representation; (b) the calculated voids (dark yellow) in the 2OED•*p*-Xy complex after guest removal, displaying the discrete cavity occupation of each guest

3.5.1 Host···host and host···guest interactions.   Complexes 2OED•*o*-Xy, 2OED•*p*-Xy and 2OED•EB experienced weak (host)π···π(host) and (host)π···π(guest) as well as (host)C–H···π(host) interactions. The latter were characterized by distances ranging between 2.62 and 2.98 Å, with accompanying angles between 86 and 164°. Strikingly, only in the 2OED•*o*-Xy complex was the guest involved in this interaction type, and one (host)C–H···π(guest) and one (guest)C–H···π(host) interaction (2.92 Å, 141° and 2.86 Å, 164°, respectively) were observed. Other short contacts were only host···host in nature: interactions (host)C–H···H–C(host), (host)N–H···N(host) and (host)C–H···N(host) ranged from 2.27 to 2.36 Å (125–165°), 2.51 to 2.59(2) Å [109.2(16)–110°] and 2.57 to 2.59 Å (102–103°), respectively. The 2OED•EB complex was also the only one that experienced a (host)N–H···H–C(host) interaction which measured 2.33 Å (137°).

Table 7 is a summary of the more significant host···guest interactions for ease of comparison. It is plausible that the two C–H···π interactions (host···guest and guest···host) between *o*-Xy and OED are responsible for the enhanced selectivity of this host for *o*-Xy relative to the other three isomers, where these intermolecular host···guest/guest···host interactions are absent. *p*-Xy and EB are merely retained in the host crystal by means of weak π···π interactions.

Table 7

Interactions	2OED•*o*-Xy	2OED•*p*-Xy	2OED•EB	Summary of the non-covalent host–guest interactions in the 2OED•*o*-Xy, 2OED•*p*-Xy and 2OED•EB complexes
(host)π···π(guest)	4.927(1)–5.842(1) Å (4 contacts)	5.459(1)–5.826(1) Å (3 contacts)	4.943(2)–5.741(2) Å (4 contacts)	
C–H···π		None	None	
(host)C–H···π(guest)	2.92 Å, 141°			
(guest)C–H···π(host)	2.86 Å, 164°			
Hydrogen bonding	None	None	None	
Other short contacts	None	None	None	

3.6 Thermal analyses

Figures 9a–c displays overlaid differential scanning calorimetric (DSC), thermogravimetric (TG) and the derivative thereof (DTG) traces that were obtained from the thermal experiments for the 2OED•o-Xy, 2OED•p-Xy and 2OED•EB complexes after heating each at 10 °C·min^{-1}. Guests were all released in a convoluted manner, and the relevant thermal data from these experiments are summarized in Table 8.

The expected guest mass loss of 8.3% for each complex was reasonably congruent with the experimental mass loss values (Table 8, 8.5% 2OED•o-Xy, 9.6% 2OED•p-Xy and 8.1% 2OED•EB). The term T_{on}–T_b, where T_{on} is the onset temperature for the guest release process and T_b the boiling point of pure guest solvent, has been suggested to be an applicable measure of the relative thermal stabilities of isostructural complexes.[28] The more positive this value, the more stable the complex is. Here, these were computed to be 2OED•o-Xy (−48.7 °C) > 2OED•p-Xy (−64.5 °C) ≈ 2OED•EB (−63.2 °C). The selectivity of OED for o-Xy is, therefore, as a result of the enhanced stability of this complex relative to the other two which is, quite plausibly, owing to the additional host···guest and guest···host interactions observed in this complex (which were absent in the other two).
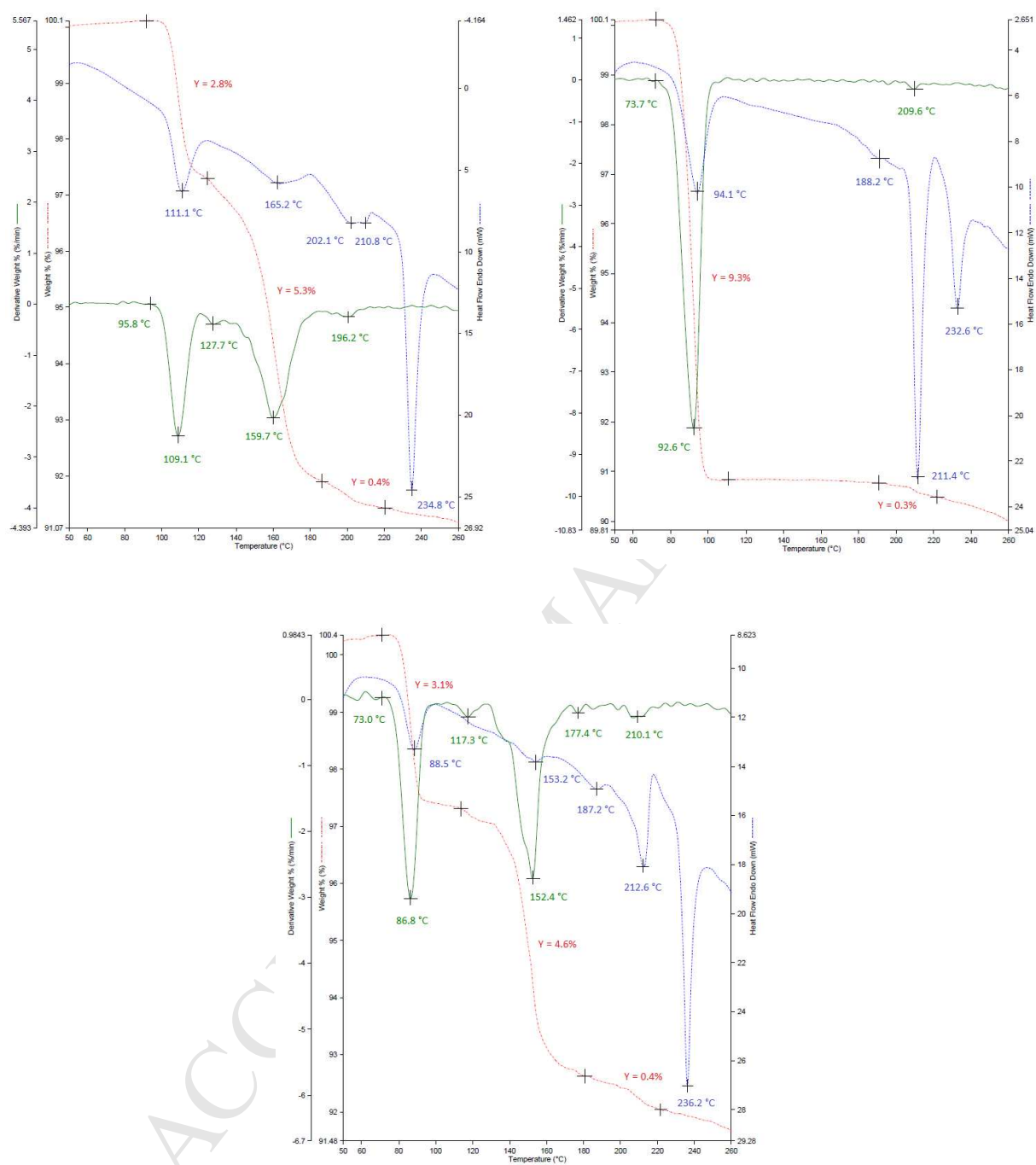
Figure 9. Thermal analyses afforded the overlaid TG (red), DSC (blue) and DTG (green) traces for the (a) 2OED•*o*-Xy, (b) 2OED•*p*-Xy and (c) 2OED•EB complexes

Table 8

Complex	T_{on} (°C)[a]	T_p (°C)[b]	T_{end} (°C)[c]	T_b (°C)	$T_{on}-T_b$ (°C)	Theoretical mass loss (%)	Observed loss (%)[d]
2OED•*o*-Xy	95.8	109.1 127.7 159.7 196.2	111.1 165.2 202.1 210.8	144.5	−48.7	8.3	8.5
2OED•*p*-Xy	73.7	92.6 209.6	94.1 188.2 211.4	138.2	−64.5	8.3	9.6
2OED•EB	73.0	86.8 117.3 152.4 177.4 210.1	88.5 153.2 187.2 212.6	136.2	−63.2	8.3	8.1

Thermal data for the 2OED•*o*-Xy, 2OED•*p*-Xy and 2OED•EB complexes

[a]T_{on} is the onset temperature for the guest release process and is estimated from the DTG trace
[b]T_p is the peak temperature obtained from the DTG trace and represents the temperature at which the rate of guest release is most rapid
[c]T_{end} is estimated from the DSC trace, and is the peak temperature for the relevant endotherms
[d]Percentage mass loss calculated from the TG trace

3.7 Conclusions

Closely related compounds OED and SED displayed very different host behaviours in the presence of each of *o*-Xy, *m*-Xy, *p*-Xy and EB. While SED did not clathrate any of these four organic solvents, OED proved successful, and formed complexes with all but *m*-Xy. Guest/guest competition experiments revealed a *o*-Xy > *p*-Xy > EB > *m*-Xy host selectivity order for OED, and no mixed complexes were formed with SED in the same conditions. The reasons for the vastly differing host behaviours was attributed to their very different geometries, in the solid state, in their cyclohexyl and xanthenyl moieties, as well as in the ethylenediamine linker. An explanation for the enhanced selectivity displayed by OED for *o*-Xy was that this guest was the only one to experience C–H⋯π interactions with OED; *p*-Xy and EB were retained in the crystal only by means of very weak π⋯π host⋯guest interactions. Furthermore, $T_{on}-T_b$ data showed that the complex containing the preferred guest also possessed an increased thermal stability relative to the other two complexes.

Supplementary information

CCDC numbers 1895818 (OED), 1895819 (SED), 18958202 (OED•*o*-Xy), 1895821 (2OED•*p*-Xy) and 1895822 (2OED•EB) contain the supplementary crystallographic data for this paper. These data can be obtained free of charge from The Cambridge Crystallographic Data Centre via www.ccdc.cam.ac.uk/data_request/cif. ^{1}H-, ^{13}C-NMR and IR spectra for all intermediates, OED and SED are also provided in the Supplementary Information, as are the ^{1}H-NMR spectrum and .cif file for the two experiments employing seed crystals.

Acknowledgements

References

1. D.J. Cram, Angew. Chem., Int. Ed. Engl. 27 (1988) 1009.

2. J.L. Atwood, G.W. Gokel, L.J. Barbour, Comprehensive Supramolecular Chemistry II, 2nd Edition, Volumes 1 and 2, Elsevier Science, Saint Louis, 2017.

3. J.W. Steed, J.L. Atwood, Supramolecular Chemistry, 2nd Edition, John Wiley & Sons, USA, 2009.

4. J.L. Atwood, J.W. Steed, Encyclopedia of Supramolecular Chemistry, Volume 1, Marcel Dekker, New York, 2004.

5. D. Seebach, A.K. Beck, A. Heckel, Angew. Chem., Int. Ed. 40 (2001) 92.

6. R.M. Kamp, D. Kyriakidis, T. Choli-Papadopoulou, Proteome and Protein Analysis, 1st Edition, Springer, Berlin, 2000.

7. J. Zheng-Yu, Cyclodextrin Chemistry: Preparation and Application, World Scientific Publishing, Singapore, 2013.

8. C.J. Egan, R.V. Luthy, Ind. Eng. Chem. 47 (1955) 250.

9. W.D. Schaeffer, W.S. Dorsey, D.A. Skinner, C.G. Christian, J. Am. Chem. Soc. 79 (1957) 5870.

10. S. F. Spencer, Anal. Chem. 35 (1963) 592.

11. E. Santacesaria, M. Morbidelli, A. Servida, G. Storti, S. Carra, Ind. Eng. Chem. Process Des. Dev. 21 (1982) 446.

12. Z-Y. Gu , X-P. Yan, Angew. Chem., Int. Ed. 49 (2010) 1477.

13. L. Alaerts, C.E.A. Kirschhock, M. Maes, M.A. van der Veen, V. Finsy, A. Depla, J.A. Martens, G.V. Baron, P.A. Jacobs, J.F.M. Denayer, D.E. De Vos, Angew. Chem., Int. Ed. 46 (2007) 4293.

14. M. Lusi, L.J. Barbour, Angew. Chem. 124 (2012) 3994.

15. J. Vicens, A.E. Armah, S. Fujii, K-I. Tomita, J. Inclusion Phenom. Macrocyclic Chem. 10 (1991) 159.

16. F. Toda, K. Tanaka, Y. Wang, G-H. Lee, Chem. Lett. 15 (1986) 109.

17. L.R. Nassimbeni, N.B. Bathori, L.D. Patel, H. Su, E. Weber, Chem. Commun. 51 (2015) 3627.

18. Y. Yang, P. Bai, X. Guo, Ind. Eng. Chem. Res. 56 (2017) 14725.

19. B. Barton, E.C. Hosten, P.L. Pohl, Tetrahedron 72 (2016) 8099.

20. B. Barton, M.R. Caira, L. de Jager, E.C. Hosten, Cryst. Growth Des. 17 (2017) 6660.

21. B. Barton, D.V. Jooste, E.C. Hosten, J. Inclusion Phenom. Macrocyclic Chem. (2019) https://doi.org/10.1007/s10847-019-00883-0

22. A. Bruker, APEX2, SAINT and SADABS, Bruker AXS Inc., Madison, WI, 2010.

23. G.M. Sheldrick, Acta Crystallogr. A 71 (2015) 3.

24. G.M. Sheldrick, Acta Crystallogr. C 71 (2015) 3.

25. C.B Hübschle, G.M. Sheldrick, B. Dittrich, J. Appl. Crystallogr. 44 (2011) 1281.

26. Mercury CSD 3.10.2 (Build 189770), http://www.ccdc.cam.ac.uk/mercury/. [Accessed 2019.]

27. Spartan' 10 V1.1.0, 2010, Wavefunction, Inc., Irvine.

28. (a)   M.R. Caira, L.R. Nassimbeni, M.L. Niven, W.-D. Schubert, E. Weber, N. Dörpinghaus, J. Chem. Soc., Perkin Trans. 2 (1990) 2129;   (b)   S.A. Bourne, L.R. Nassimbeni, E. Weber, K. Skobridis, J. Org. Chem. 57 (1992) 2438; (c)   L.J. Barbour, M.R. Caira, L.R. Nassimbeni, J. Chem. Soc., Perkin Trans. 2 (1993) 1413.